

## High resolution SXR emissivity and two foil $T_e$ characterization in RFX-mod helical states

A.Ruzzon, A.Fassina, P.Franz, M.Gobbin and L.Marrelli

*Consorzio RFX – Associazione Euratom-ENEA – Padova, Italy*

**Single Helical Axis in RFX-mod.** In the Reversed Field Pinch (RFP) configuration the plasma can access the Quasi Single Helicity (QSH) regime [1] where one single mode dominates the magnetic perturbations spectrum and a magnetic island appears; for sufficiently large amplitude of the dominant mode (in the RFX-mod experiment the one with poloidal and toroidal number  $m=1$ ,  $n=7$  respectively) the island separatrix is expelled, hence the magnetic topology is characterized by a single helical magnetic axis. These states are labelled SHAx (Single Helical Axis) and they are characterized by a helically symmetric core plasma within electron internal transport barriers (ITBs) [2].

SHAx structures have been initially detected and analysed thanks to the high spatial resolution Thomson scattering diagnostic. This study has allowed a good characterization of the electron temperature radial profile and of its gradient but the poor temporal resolution prevented to follow the time evolution of these helical structures during the discharge. Such a limitation has recently been overcome by using high frequency resolution Soft X Rays (SXR) diagnostics.

By this work we present the first results from the new SXR diagnostics in RFX-mod, dedicated to reconstruct the electron temperature evolution profile with a high time resolution allowing a careful study of the SHAx states dynamic.

**SXR diagnostics.** The RFX-mod experiment is provided with three SXR diagnostics with a sampling capability up to 10 kHz which detect the integral (brightness), along different sight lines, of the plasma SXR emissivity. The SXR tomography, placed at the toroidal angle

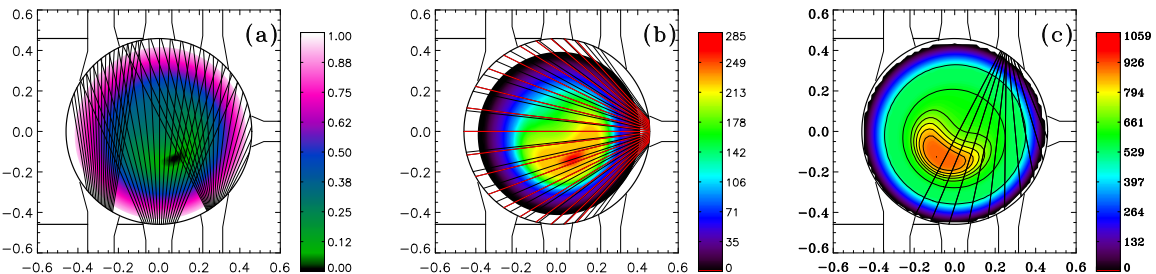


Fig. 1: Examples of helical equilibria reconstructions on the poloidal section: a)  $\rho$  map at  $\phi=202^{\circ}30'$ ; in black: the tomography vertical sight lines; b) emissivity map at  $\phi=202^{\circ}30'$  obtained with the convergence algorithm; in black and the red: the tomography horizontal sight lines; c) temperature map at the multi-camera position  $\phi=262^{\circ}30'$ : the helical structure has changed position with the (1,-7) periodicity; in black: the multicamera diagnostic sight lines.

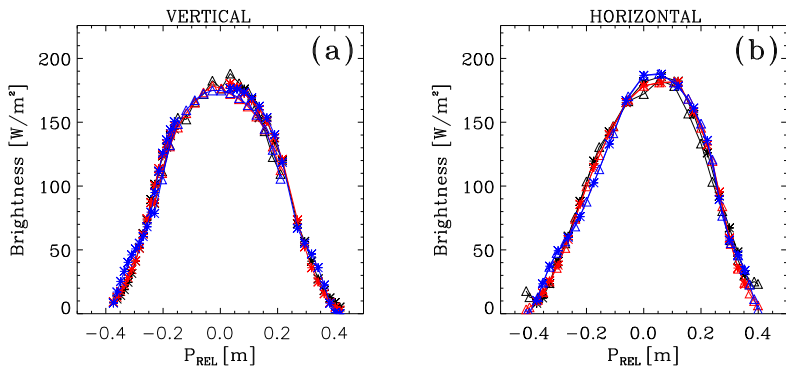


Fig. 2: Brightness data example for horizontals and verticals tomography arrays (#28920, t=112ms): in black the experimental data, in red the integration along the sight lines of the convergence algorithm emissivity and in blue the integration along the sight lines of the temperature profile emissivity.

$\phi=202^{\circ}30'$ , is composed by 103 sight lines with the same Beryllium filter thickness (42  $\mu\text{m}$ ), split in 5 arrays: 3 vertical (57 sight lines as shown in fig.1a by the vertical straight line) and 2 horizontal (46 sight lines as shown in fig.1b by the red and black straight lines). An other horizontal array of 19 sight lines (the red straight lines in fig.1b) with a different Beryllium filter thickness (88  $\mu\text{m}$ ) is used to compute the electron temperature by the two-foil technique [3]. Finally, a SXR multi-camera diagnostic, placed at the toroidal angle  $\phi=262^{\circ}30'$ , allows to determine the electron temperature, by the two-foil technique, along 10 sight lines (shown in fig.1c by the straight lines).

**Brightness and emissivity profiles.** SHAx states are described by using a suitable system of flux coordinates which takes into account the helical deformation of the plasma [4]. To this end a new coordinate  $\chi$  has been defined in such a way to be constant on the helical flux surfaces, thus satisfying the equation  $B \cdot \nabla \chi = 0$  with  $\chi$  given by:

$$\chi = (\psi_{0P} - 7\psi_{0T}) + (\psi_{7P} - 7\psi_{7T}) \cos(\theta^* - 7\phi + \varphi) \quad (1)$$

where  $\psi_{0T}$  is the unperturbed axisymmetric toroidal magnetic flux,  $\psi_{0P}$  is the unperturbed axisymmetric poloidal magnetic flux,  $\psi_{7T}$  and  $\psi_{7P}$  are the (1,-7) component of the toroidal and poloidal magnetic flux perturbations respectively. In the following, for the sake of simplicity, we use as helical flux function the square root of  $\chi$  normalized to its maximum value:  $\rho = (\chi/\chi_{max})^{1/2}$ . A map of  $\rho$  reconstruction on a poloidal section is shown in fig.1a where the helical geometry is clearly visible.

The SXR emissivity  $\varepsilon$  is assumed to be a function only of helical coordinate,  $\varepsilon = \varepsilon(\rho)$ ; a numerical algorithm has been developed to find the best function  $\varepsilon(\rho)$  that reproduces, by the integration

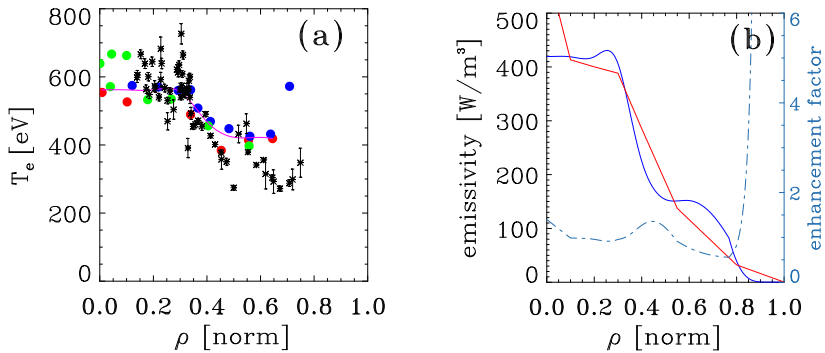


Fig. 3: a) Example of temperature profiles (#28920,  $t=112\text{ms}$ ): the green dots are the measurements from the multicamera, in blue and red from the two foil tomography diagnostic; blue and red are relative the two sides of the helical structure; the Thomson scattering measurements are plotted with the black marks. b) Examples of emissivity (#28920,  $t=112\text{ms}$ ): in red the profile from the convergence algorithm, in blue from the temperature profile; the dotted line identifies the enhancement factor.

along the sight lines, the experimental brightness. As initial guess  $\varepsilon(\rho)$  is chosen to be a broken line with 7 emissivity values at fixed  $\rho$  positions: the algorithm, based on a minimum  $\chi^2$ -square method, change automatically the shape until the best fit with the experimental brightness is reached. The profile of  $\varepsilon(\rho)$  is imposed to be monotonically decreasing and null at the edge, i.e.  $\varepsilon(\rho=1)=0$ .

Fig.2 shows the good matching between the experimental (in black) and the simulated values of brightness (in red) which validates the initial assumption to describe the plasma topology in terms of helical equilibrium with constant emissivity  $\varepsilon(\rho)$  on the flux surfaces

**Electron temperature profile.** The relation between the electron temperature and the SXR emissivity is given by:

$$\varepsilon(T_e) = K \int_E dE \frac{n_e^2}{\sqrt{T_e}} e^{\frac{-E}{T_e}} T_{Be}(E) A_{Si}(E) \quad (2)$$

where  $T_e$  is the electron temperature,  $n_e$  is the electron density,  $T_{Be}(E)$  is the Beryllium filter transmission function,  $A_{Si}(E)$  is the Silicon detector absorption function,  $E$  is the energy of the photon emission and  $K$  is a constant which takes into account the contributions of recombination and line radiation to the electron bremsstrahlung emission.

An independent determination of the emissivity profile  $\varepsilon'(T_e(\rho))$  has been computed by using Eq. (2) and the electron temperature profile  $T_e(\rho)$  obtained from the two foil SXR diagnostic.

Results are reported in Fig.3a: the dots correspond to the electron temperatures collected by the two-foil diagnostic while the dashed line to the corresponding  $T_e(\rho)$  profile developed from these

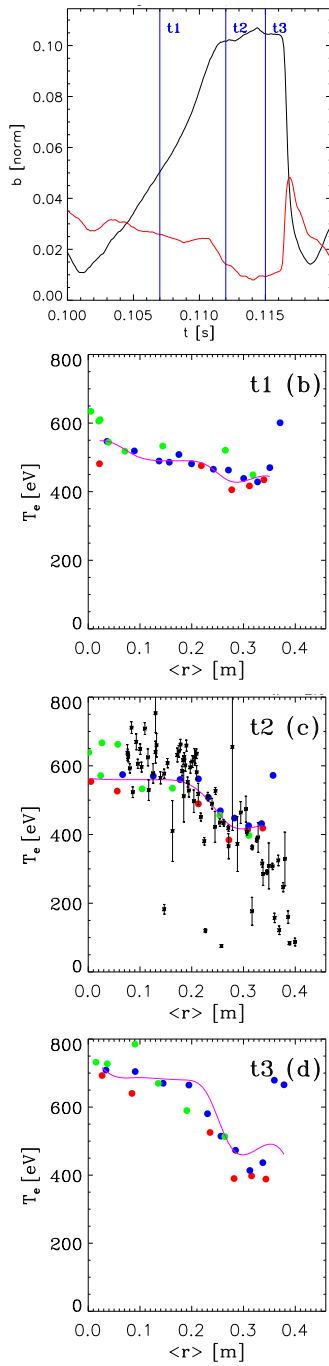


Fig. 4: Temperature profile evolution (#28920): a) the magnetic perturbations in normalized scale versus time, in black the dominant mode and in red the secondary ones; b) the temperature profile at 107ms; c) at 112ms; d) at 115ms.

data. Fig.3b shows the emissivity generated by this temperature profile (with a red line) and fig.2 reports the brightness with blue lines together with the one from previous simulations (red) and the experimental data (black).

The ratio between the emissivity profile  $\varepsilon(\rho)$  and  $\varepsilon'(T_e(\rho))$  gives an estimate of the enhancement factor  $\xi(\rho)$ , reported in fig.3b with a dotted line;  $\xi(\rho)$  furnishes an evaluation of the recombination and line radiation contribution. Up to now  $\xi(\rho)$  is characterized by a variable shape.

The  $T_e(\rho)$  profile allows to study the electron temperature gradient evolution during the QSH regimes. To have a more physical radial coordinate,  $\rho$  is converted into an effective radius  $\langle r \rangle$  defined as  $\langle r \rangle = \sqrt{S(\rho)/\pi}$ , where  $S(\rho)$  is the flux surface area. In fig.4 a sequence of  $T_e(\langle r \rangle)$  is illustrated; in this example the temperature gradient changes during the discharge, in particular it increases with the growing of the dominant mode and with the decreasing of the secondary modes. This behavior appears to be common to all the analyzed cases; in particular, the amplitude of the secondary modes plays the most important role in determining the shape of the electron temperature gradient. Such a correlation between the magnetic modes and the  $T_e$  profiles is currently under investigation by considering a larger database of experimental RFX-mod plasmas.

- [1] Martin P. et al., Phys. Control. Fusion **49**, A177 (2007)
- [2] Lorenzini R. et al., Phys. Rev. Lett. **101**, 025005 (2008)
- [3] Bonomo F. et al., Rev. Sci. Instrum. **77**, 10F313 (2006)
- [4] Momo B. et al., Proceedings of the 37th EPS Conference on Plasma Physics, Dublin, 21 - 25 June 2010, P4.147